(ii) *The hydrogen-bonding system*

The molecules possess a possible donor in the hydroxyl group O(4)–H(O4) and possible acceptors in O(5) and the two anhydro oxygen atoms O(23) and O(16). The hydrogen-bonding scheme and its distances and angles are shown in Table 4 and Figs. 4 and 5. O(16) is not involved in hydrogen bonds at all, the closest intermolecular O(4)–O(16) distance being 3·85 Å.

The two independent molecules are not hydrogen-bonded to each other, but form two entirely separate bonding systems. In all molecules 1, atoms O(23) are the acceptors for hydrogen bonds of 2·87 Å length, by which the molecules are connected to infinite chains around the screw axis parallel to **a**. In all molecules 2, atoms O(5) play the roll of acceptors for hydrogen bonds of 2·97 Å length, by which the molecules are connected to infinite chains around the screw axes parallel to **b**. The next shortest O(4)–O distances are 3·27 and 3·32 Å. Even if they are considered as very weak hydrogen bonds, they do not form bonds between molecules 1 and molecules 2. Besides, there is no evidence for intramolecular hydrogen bonding.

The existence of 40 intermolecular distances smaller than 3·0 Å (not including those which are involved in hydrogen bonding) suggests strong van der Waals interactions between the molecules. The minimum values of 2·40 and 2·54 Å for H–H and O–H distances, respectively, are close to the sum of the van der Waals radii ($r_O = 1{\cdot}4$, $r_H = 1{\cdot}2$ Å).

This research is supported in part by the U.S. Public Health Service, National Institutes of Health, under Grant Nos. GM-11293, GM-01728 and NS-02763. The IBM 7090 and 1130 computer programs were modified and adapted by Dr R. Shiono. We wish to thank Professor G. A. Jeffrey for his encouragement and helpful suggestions during the course of this work, Dr R. Rosenstein for suggesting the problem, and Dr C. Levinthal for use of his ADAGE computer. We are grateful for the skillful technical assistance of Mrs Joan Klinger.

### References

BERMAN, H. M. & KIM, H. S. (1968). *Acta Cryst.* B**24**, 897.
BROWN, G. M. & THIESSEN, W. E. (1969). *Acta Cryst.* A**25**, S195.
CARVALHO, J. S., PRINS, W. & SCHUERCH, C. (1959). *J. Amer. Chem. Soc.* **81**, 4054.
*International Tables for X-ray Crystallography* (1962). Vol. III. Birmingham: Kynoch Press.
ISAACS, N. W. & KENNARD, C. H. L. (1970). *Chem. Commun.* p. 360.
JOHNSON, C. K. (1965). Technical Report ORNL 3794, Oak Ridge National Laboratory, Oak Ridge, Tennessee.
NORDMAN, C. E. (1966). *Trans. Amer. Cryst. Assoc.* **2**, 29.
PARK, Y. J., KIM, H. S. & JEFFREY, G. A. (1970). *Acta Cryst.* B**27**, 220.
RUTHERFORD, J. S. (1968). Unpublished work.
SCHOMAKER, V. & TRUEBLOOD, K. N. (1968). *Acta Cryst.* B**24**, 63.
SEEMAN, N. C. (1970). Technical Report TR-70-1. Department of Crystallography, Univ. of Pittsburgh.
SHIONO, R. (1968). Unpublished work.
SHIONO, R. (1969). Unpublished work.
STEWART, R. F., DAVIDSON, E. R. & SIMPSON, W. T. (1965). *J. Chem. Phys.* **42**, 3175.

*Acta Cryst.* (1971). B**27**, 1760

# The Effect of Molecular Vibrations on Apparent Bond Lengths. II. Water Molecule

BY M. W. THOMAS

*Mathematical Institute, Oxford University, OX1 3LB, England*

(*Received* 2 *March* 1971)

The apparent contraction of the O–H bond in $H_2O$ due to the nuclear vibrational motion has been studied using a convolution approximation with both Slater- and Gaussian-type wave functions. The bond length here is taken as the distance between the maxima in the charge density such as would be inferred from X-ray measurements. The predicted degree of contraction appears to be quite sensitive to the quality and type of wave function used. The Gaussian function did not adequately represent the charge density near the hydrogen nucleus. However, the best Slater-type wave function gave a bond contraction of 0·13 $a_0$. Difference densities were also investigated and an estimate was made of the contribution to the bond shortening from the bending motion alone.

## Introduction

It is well known (Dawson, 1965) that bond lengths to terminal hydrogen atoms as determined by X-rays are generally smaller than those determined by spectroscopic or neutron- and electron-diffraction methods. In a previous paper (Coulson & Thomas, 1971), which henceforth will be referred to as I, we have shown that some of this apparent shortening can be accounted for by considering the effect of the nuclear vibrational motion on the electronic charge density associated with the equilibrium molecular geometry. In general, the

vibrational motion will smooth out the 'cusps' in the charge density at the nuclei. However, if the charge density near the nucleus is sufficiently aspherical and the vibrational motion is nearly harmonic then the peaks in the charge density will not correspond to the positions of the nuclei.

Generally, the asphericity of the charge density near a nucleus will be due to the effects of bonding. Moreover, as Coulson (1970) has pointed out, the asphericity will be greatest for atoms whose 1*s* electrons are involved in bonding. Indeed, as shown in I, the effect is significant for certain diatomic molecules such as $H_2$ and $H_2^+$, where the bond shortenings are of the order of 0·1 $a_0$.

In the case of polyatomic molecules, one would again expect an apparent shift in the position of a terminal hydrogen atom due to the effect of the vibrational motion on the aspherical electron charge at the nucleus. However, unlike diatomics, the internal vibrational motion will include bending as well as stretching modes. As pointed out by Cruickshank (1956) and Dawson (1967), librational motions alone cause apparent bond shortenings, even for atoms with spherical charge distributions. But if there is charge asphericity in the direction of the bending motion, then bending motions will result in apparent bond angles different from the equilibrium values. It should be noted that this 'apparent bond angle' effect can also occur from anharmonic vibrational but not from anisotropic harmonic motions. However, to study these effects in detail, it is necessary to have good wave functions and a completely determined vibrational potential function. For these reasons calculations were performed on the water molecule.

As vibrational amplitudes are small compared with the equilibrium bond lengths and valence angles the convolution approximation discussed in I was used throughout. So we write

$$\varrho_{H_1}(\mathbf{R}) = \int P_{H_1}(\mathbf{r})\varrho_{eq}(\mathbf{R}-\mathbf{r})d\mathbf{r} \qquad (1)$$

where $P_{H_1}(\mathbf{r})$ is the marginal probability density [see equation (10)] describing the vibrational motion of the hydrogen atom, $H_1$. The static electron density $\varrho_{eq}$ is taken at the equilibrium geometry for which wave functions near the Hartree–Fock (H–F) limit were used. The resulting dynamic density for the hydrogen atom is denoted by $\varrho_{H_1}(\mathbf{R})$. It should be pointed out that $\varrho_{H_1}(\mathbf{R})$ is strictly valid only in a region near the $H_1$ equilibrium position as the integral only reflects the $H_1$ dependence. However, this is not too serious as the oxygen atom has a small vibrational amplitude due to its greater mass. In fact, in a more sophisticated treatment it would be necessary to know the static wave function as a continuous function of the molecular geometry. Such wave functions are not yet available for water.* Moreover, in I the results for $H_2^+$ indicated that the convolution approximation was a good approximation for the exact Born–Oppenheimer density.

The purpose of this paper, then, is to examine the magnitude of the apparent bond shortening within the convolution approximation of equation (1) for various wave functions for an isolated water molecule. In order to estimate the contributions to the apparent bond shortening from the bending motion a calculation was also made using a 'bending only' vibrational distribution function, $P_{H_1}(\mathbf{r})$, in equation (1). This function, $P_{H_1}(\mathbf{r})$, was calculated on the assumption that the oxygen atom remained at rest and that the motion of the hydrogen atom $H_1$ was due only to the vibrational bending mode.

## Vibrational motion

Although the vibrational potential energy function $V(r_1\, r_2\, \theta)$ for an isolated water molecule can be easily determined within the harmonic approximation (Wilson, Decius & Cross, 1955), certain difficulties of interpretation arise when anharmonic potential functions are used (Pliva, 1963; Kuchitsu & Morino, 1965; Kuchitsu & Bartell, 1962). These difficulties arise partly because the potential energy should be expressed as a function of the internal coordinates and these depend non-linearly on the Cartesian coordinates, and also partly because the various constants in the potential function are now not all determined by the available experimental data. Since the interest here lies in the extent to which the asphericity of a terminal hydrogen atom can lead to apparent bond length changes it suffices to use the harmonic approximation for the vibrational motion. In fact, since anharmonic oscillator wave functions are usually expanded as a perturbation in a basis of harmonic oscillator wave functions, the major contribution to the nuclear distribution would come from the harmonic terms.

To compute the harmonic probability distribution $P_{H_1}(\mathbf{t})$ the well known F–G matrix formulation was used (Wilson, Decius & Cross, 1955). The force constants for the internal symmetry coordinates are listed in Table 1 together with the other molecular constants. The G matrix (kinetic energy matrix) was calculated using the atomic masses and the known equilibrium molecular geometry. The internal displacement coordinates $\mathbf{p}$, $(p_1,p_2,\theta)$ were taken to be linear combinations of the in plane Cartesian displacement coordinates $\mathbf{r}$, $(r_{x_i} r_{y_i}, i=1,2,3)$

$$\mathbf{p} = \mathsf{T}\cdot\mathbf{r} \qquad (2)$$

where T is a $3\times 6$ matrix. The internal coordinates $\mathbf{p}$ were then transformed to internal symmetry coordinates $\mathbf{s}$ by a unitary transformation U

$$\mathbf{s} = \mathsf{U}\cdot\mathbf{p}\,. \qquad (3)$$

The latent roots of the G·F matrix were then obtained, and hence the non-zero normal frequencies $\Lambda$, the normal modes $\mathbf{q}$ and also a non-singular transformation L

* Kern (1970) has recently computed part of the potential energy surface for water.

back to the symmetry coordinates

$$\mathbf{s}=\mathsf{L}\cdot\mathbf{g}\,. \tag{4}$$

However, for the isolated water molecule this procedure also leads to three zero frequencies corresponding to the three linear relations defined by the Eckart (1935) conditions

$$\mathsf{C}\cdot\mathbf{r}=0 \tag{5}$$

where C is a $3\times6$ non-singular matrix. These conditions arise from choosing a non-rotating frame of reference fixed at the molecular centre of mass. Equations (5) and (2) can be used to eliminate three Cartesian displacement coordinates, leaving only the coordinates of the hydrogen atom $(h_1, h_2)$ and some other Cartesian displacement coordinate $\alpha$. Hence equation (2) can be written as

$$\mathbf{p}=\mathsf{B}\cdot\mathbf{t}\,. \tag{6}$$

From equations (3), (4) and (6) one can construct a non-singular linear transformation from $\mathbf{t}=(h_1, h_2, \alpha)$ to the normal coordinates $\mathbf{q}=(q_1, q_2, q_3)$

$$\mathbf{q}=\mathsf{P}\cdot\mathbf{t} \tag{7}$$

where $\mathsf{P}=\mathsf{L}^{-1}\cdot\mathsf{U}\cdot\mathsf{B}$ is a non-singular $3\times3$ matrix. For the ground vibrational state the nuclear wave function is

$$\psi(q)=\varphi^0_{\lambda_1}(q_1)\varphi^0_{\lambda_1}(q_2)\varphi^0_{\lambda_1}(q_3) \tag{8}$$

where each $\varphi^0_{\lambda i}(q_i)$ is a ground-state harmonic oscillator function. Implicit in equation (8) is the assumption that the phases between the $q_i$ are random. Then by means of equations (6) and (7) the probability density for $\mathbf{t}$ can be written as

$$\varrho(\mathbf{t})=\psi^2(\mathsf{P}\cdot\mathbf{t})\det(\mathsf{P})\,. \tag{9}$$

Finally the nuclear probability density for the hydrogen atom $H_1$ is

$$P_{H_1}(h_1,h_2)=\int\varrho(\mathbf{t})\mathrm{d}\alpha$$
$$=A\exp\{-(D_1h_1^2+D_{12}h_1h_2+D_2h_2^2)\}. \tag{10}$$

The constants $A$, $D_1$, $D_{12}$, and $D_2$ are listed in Table 1. In a similar way equation (5) was used to obtain an expression for $P_O(o_1,o_2)$, the nuclear probability density for the oxygen atom, with in-plane coordinates $(o_1,o_2)$. However, owing to its larger mass the oxygen atom has a very much smaller vibrational amplitude; in fact, without serious error it can be considered to be at rest relative to the centre of mass.

For the bending calculation the $F_{22}$ constant of Table 1 was used together with $r_e$ to compute the displacement perpendicular to the O–H bond. The oxygen atom was taken to remain stationary and each hydrogen was assumed to contribute equally to the change in bond angle. With these assumptions $P_H(h_1\,h_2)$ was computed and used in equation (1).

In these calculations only the ground vibrational state was considered as it is the only state that is appreciably populated at room temperature.

Table 1. *Molecular constants*

| | |
|---|---|
| Molecular geometry* | |
| $r_e$ | 1·8111 $a_0$ |
| $\theta$ | 104°31′ |
| Harmonic force constants† | |
| $F_{11}$ | 8·3528 mdyne. $a_0^{-1}$ |
| $F_{12}$ | 0·3217 |
| $F_{22}$ | 0·7605 |
| $F_{33}$ | 8·5545 |
| Harmonic frequencies | |
| $\lambda_1$ | 3832·01 $cm^{-1}$ |
| $\lambda_2$ | 1648·86 |
| $\lambda_3$ | 3942·55 |
| Calculated constants | |
| $A$ | 10·188523 $a_0^{-2}$ |
| $D_1$ | 31·834499 |
| $D_2$ | 32·385669 |
| $D_{12}$ | 5·082053 |

* Benedict, Gailer & Plyler (1956)
† Kuchitsu & Partell (1962)

## Results for various electronic wave functions

The static electron charge density $\varrho_{eq}$ used in equation (1) was computed from various wave functions calcul-

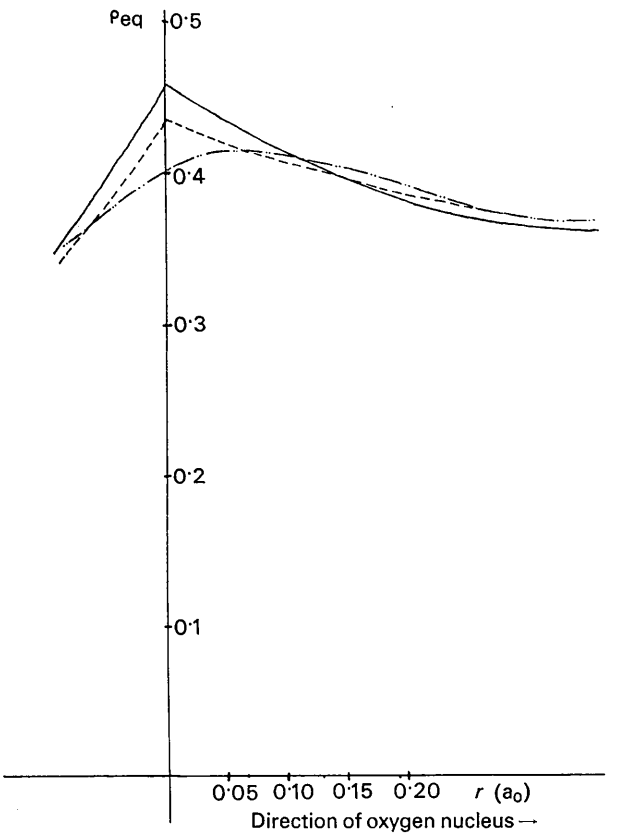


Fig. 1. Static charge density $\varrho_{eq}$ along the O–H bond axis for various wave functions. ———— STOB (Arrighini *et al.*, 1970). ---------- STOA (Aung *et al.*, 1968). ··—·—·· GTO (Neumann & Moskowitz, 1968).

ated at fixed molecular geometries close to the spectroscopic geometry. Data for the three wave functions used are summarized in Table 2. Two used Slater-type orbitals (STO's) and one used contracted Gaussian orbitals (CGTO's). In all cases, only a single configuration ($1a_1^2$, $2a_1^2$, $1b_2^2$, $3a_1^2$, $1b_1^2$) was utilized. However, since extensive basis sets, including *d* orbitals, were used all the wave functions are close to the H–F limit. One would expect that computed one-electron properties such as the charge density should be reasonable well represented by such wave functions. The first wave function, labelled STOA, was computed at the spectroscopic equilibrium geometry by Aung, Pitzer & Chan (1968). The second, labelled STOB (Arrighini, Guidotti & Salvetti, 1970), used two more basis functions on the oxygen and hence has a slightly better energy. The third, labelled GTO (Neumann & Moskowitz, 1968), has the best energy. However, it uses orbitals which are built up from Gaussian-type functions. Unfortunately, these are known to be poor at representing the wave function near the nucleus. This is vividly illustrated in Fig. 3 where the local maxima of the static density $\varrho_{eq}$ occur not at the hydrogen nuclei but are shifted into the bond. This suggests that even Gaussian-type wave functions close to the H–F limit may not represent the charge density adequately near the hydrogen nucleus. Also, one can see from Fig. 1 that the charge density calculated from STOA differs from that calculated from STOB even though their energy difference is small. Both these points indicate that substantial differences in the charge density near the hydrogen atoms make little difference to the total energy.

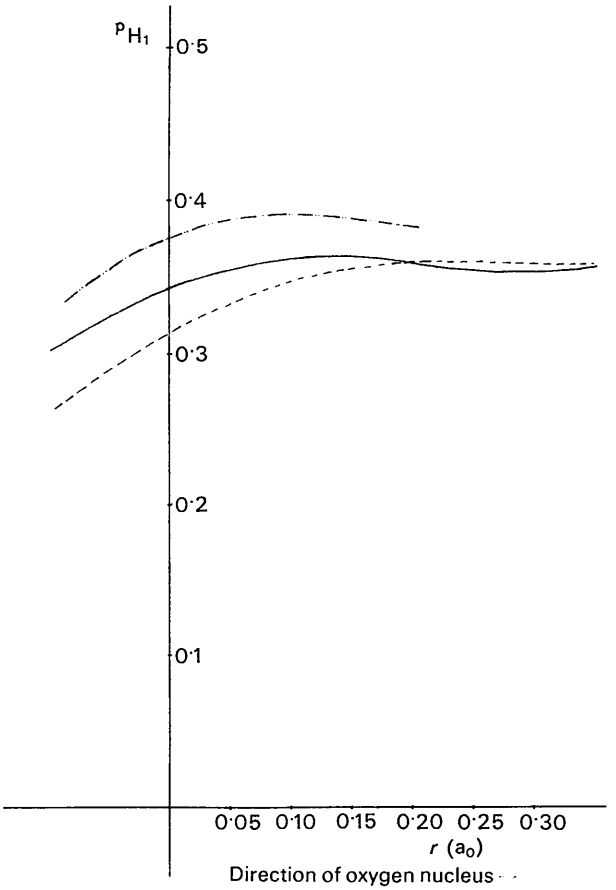


Fig. 2. Dynamic charge density $\varrho_{H1}$ along the O–H bond axis. ———— Dynamic density using STOB. ---------- Dynamic density using STOA. ··—··—·· Dynamic density using STOB and a 'bending only' vibrational distribution.

Table 2. *Wave function data*

| | STOA | STOB | GTO |
|---|---|---|---|
| Geometry | | | |
| $r$ ($a_0$) | 1·811 | 1·8103 | 1·80 |
| $\theta$ (°) | 104·25 | 105 | 105 |
| Basis set size | | | |
| STO | 25 | 27 | — |
| CGTO | — | — | 31 |
| Energy ($a_0$) | −76·0047 | −76·0384 | −76·0440 |
| Electron density at hydrogen nucleus (e.$a_0^{-3}$) | 0·437 | 0·459 | 0·404 |

The resulting dynamic electron density $\varrho_{H_1}(\mathbf{r})$ for the two STO wave functions is shown in Fig. 2. In both cases the origin is taken at the hydrogen nucleus and the electron density is plotted along the bond axis. For the STOA wave function there is really only a shoulder in the charge density $\varrho_H(\mathbf{r})$. The STOB wave function, however, has a clearly defined local maximum which is shifted towards the oxygen atom to give an apparent bond shortening. These results are listed in Table 3.

Table 3. *Displacements of the maximum of the charge density*

(Origin is taken at the hydrogen nucleus; all shifts are in the direction of the oxygen nucleus; units are $a_0$)

| | STOB | | STOA |
|---|---|---|---|
| | Total vibration | Bending only | |
| Displacement ($a_0$) | 0·13 | 0·10 | shoulder only |
| Charge density at maximum (e.$a_0^{-3}$) | 0·362 | 0·391 | 0·360 |
| Displacement of difference density ($a_0$) | 0·10 | — | 0·12 |

The STOB wave function was also convoluted with a 'bending only' vibrational function. The results are plotted in Fig. 2 and the shift is given in Table 3.

It is also instructive to examine the contribution to $\varrho_H(\mathbf{r})$ from the oxygen atomic density $\sigma_O(\mathbf{r})$. Of course there is no unique choice of $\sigma_O(\mathbf{r})$. It could be a free oxygen atom centred at the oxygen nucleus, or polarized or partially ionized with either a spherical or a

non-spherical charge density. However, for purposes of comparison it is convenient to take a spherically symmetric 'free atom' charge density. This was computed from a ground state wave function near the H–F limit (Bagus & Gilbert, 1967). The positions of the peaks for this difference density are listed in Table 3. In Fig. 3 the difference density, $\varrho_H - \sigma_O$ has been plotted for the STOB wave function along the bond axis. For comparison the dynamic density $\varrho_H(\mathbf{r})$ and the static charge density $\varrho_{eq}(\mathbf{r})$ are also plotted. From the diagram one sees that an appreciable part of $\varrho_H$ comes from the charge density of the oxygen atom $\sigma_O$ even near the hydrogen nuclei.

## Conclusions

Perhaps the most interesting result is the sensitivity of the charge density near the nucleus to the type of wave function. Although the two Slater-type wave functions give comparable electron densities the Gaussian-type wave function misplaces the peak in the charge density despite the fact that the wave function is close to the H–F limit. Since only one simple polyatomic molecule has been considered it is difficult to say whether Gaussian-type functions will generally misrepresent the charge density near the hydrogen nuclei. If this were so it would be difficult to compute bond shortenings for more complicated molecules as Gaussian wave functions are usually the only ones presently available.

The effect of the vibrational motion is to smear out the peak in the charge density at the hydrogen nucleus In the case of the STOA wave function the peak at the hydrogen is reduced to a shoulder on the charge density. However, for the STOB wave function a slight peak remains. The fact that the peak is broadened and almost disappears illustrates the difficulty in deciding what to take as the apparent bond length. Nevertheless, if one subtracts the charge density due to a spherical oxygen atom, peaks are obtained corresponding to bond shortenings of 0·1 $a_0$ for STOB and 0·12 $a_0$ for STOA. These are comparable with apparent bond length shortenings found in measurements of O–H bonds (Hamilton & La Placa, 1968). Also it is interesting to note in Fig. 3 the appreciable contribution to the charge density at the hydrogen nuclei from the oxygen atom. Moreover, the degree of contribution will depend on the shape and location of the oxygen density function. In the discrete atom model, in which the total molecular density is taken to be the sum of the atomic densities, these considerations will affect the bond length measurements.

The apparent bond shortening of 0·1 $a_0$ for the bending motion alone was less than the shortening of 0·13 $a_0$ for the total vibrational motion of the isolated molecule. One would expect the total vibrational motion to show a larger shift as the stretching modes alone should produce an apparent bond shortening as was shown in I. However, the small difference between the two shortenings is probably not the total stretching mode contribution as the 'bending only' calculation used just the $F_{22}$ force constant of Table 1. In the actual molecule there is an $F_{12}$ force constant which couples the bending motion with the symmetric stretching mode. In fact in a water molecule in ice there is a great deal of coupling between the intermolecular modes of neighbouring molecules as well as coupling with the lattice modes (Eisenberg & Kauzmann, 1970). Unfortunately, the potential function for such a system is not yet available.

I would like to thank Shell Canada for their generous financial grant. Also I am deeply indebted to Professor C. A. Coulson for suggesting this work and for his enthusiastic encouragement and helpful discussions.

## References

ARRIGHINI, C. P., GUIDOTTI, C. & SALVETTI, O. (1970). *J. Chem. Phys.* **52**, 1037.

AUNG, S., PITZER, R. M. & CHAN, S. I. (1968). *J. Chem. Phys.* **49**, 2071.

BAGUS, P. S., & GILBERT, T. L. (1967). Tables from *IBM Journal of Research, Supplement.* Edited by A. D. MCLEAN & M. YOSHIMINE.

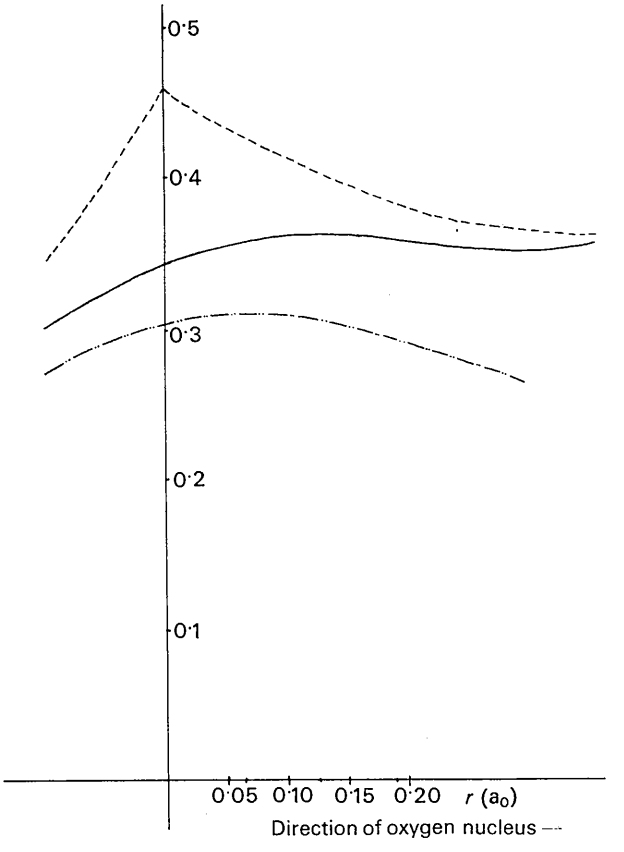


Fig. 3. Axial density for $H_2O$ using STOB. ---------- Static density $\varrho_{eq}$. ———— Dynamic density $\varrho_{H_1}$. ··—··—·· Difference density $\varrho_{H_1} - \sigma_O$.

BENEDICT, W. S., GAILAR, N. & PLYLER, E. K. (1956). *J. Chem. Phys.* **24**, 1139.
COULSON, C. A. (1970). *Thermal Neutron Diffraction.* Edited by B. T. M. WILLIS. Oxford Univ. Press.
COULSON, C. A. & THOMAS, M. W. (1971). *Acta Cryst.* B**27**, 1354
CRUICKSHANK, D. W. J. (1956). *Acta Cryst.* **9**, 757.
DAWSON, B. (1965). *Aust. J. Chem.* **18**, 595.
DAWSON, B. (1967). *Proc. Roy. Soc.* A**298**, 255.
ECKART, C. (1935). *Phys. Rev.* **47**, 552.
EISENBERG, D. & KAUZMANN, W. (1969). *The Structure and Properties of Water.* Oxford Univ. Press.
HAMILTON, W. C. & LA PLACA, S. J. (1968). *Acta Cryst.* B**24**, 1147.
KERN, C. W. (1970). Private communication.
KUCHITSU, K. & BARTELL, L. S. (1962). *J. Chem. Phys.* **36**, 2460.
KUCHITSU, K. & MORINO, Y. (1965). *Bull. Chem. Soc. Japan*, **38**, 814.
NEUMANN, D. & MOSKOWITZ, J. W. (1968). *J. Chem. Phys.* **49**, 2056.
PLIVA, J. & CIHLA, Z. (1963). *Coll. Czech. Chem. Commun.* **28**, 1232.
WILSON, E. B., DECIUS, J. C. & CROSS, P. C. (1955). *Molecular Vibrations.* New York: McGraw-Hill.

*Acta Cryst.* (1971). B**27**, 1765

# Refinement of the Crystal Structure of Ferroelectric Acid Lithium Selenite: Position of the Lithium Ion

BY J. K. MOHANA RAO AND M. A. VISWAMITRA
*Department of Physics, Indian Institute of Science, Bangalore-12, India*

(*Received* 10 *November* 1969 *and in revised form* 2 *November* 1970)

The lithium ion in the ferroelectric acid lithium selenite (not obtained in the original X-ray work of Vedam, Okaya & Pepinsky) has been located at the pseudoinversion centre $(\frac{1}{2},\frac{3}{4},0)$ from considerations of symmetry, crystal chemistry and model building. This position is confirmed from three-dimensional Fourier and difference Fourier syntheses, the peak height at the lithium ion site being three times the standard deviation in the electron density. The lithium ion is coordinated octahedrally to six non-equivalent selenite-oxygen atoms. The hydrogen positions have been proposed on the basis of bond-length and bond-angle criteria. They indicate that the selenite groups containing Se(1) and Se(2) have respectively the structures $H_2SeO_3$ and $HSeO_3^-$.

## Introduction

Pepinsky & Vedam (1959) first reported that acid lithium selenite, $LiH_3(SeO_3)_2$, abbreviated hereafter as ALS, is a room-temperature ferroelectric. It melts at 110°C before a Curie point is reached. It is the only soft ferroelectric known so far to exhibit an appreciably high value of spontaneous polarization, $P_s$, *viz.* 15 microcoulomb.cm$^{-2}$ (Jona & Shirane, 1962). The direction of $P_s$ is in the mirror plane, approximately normal to (001) (Pepinsky & Vedam, 1959; Berlincourt, Cook & Rander, 1963). The mechanism of polarization reversal in ALS single crystals was studied by Fatuzzo (1959 and 1960). Berlincourt and his colleagues, besides dielectric studies, reported investigations on the piezo- and pyro-electric, as well as the elastic, properties of this crystal. Recently, a ferro- to para-electric transition at 72°C was induced in ALS by the application of a hydrostatic pressure of 12·5 kbar, which indicated a hypothetical Curie point of 147°C (Samara & Anderson, 1966; Samara, 1968). ALS was also the first crystal with point group *m* to show rotatory power along its optic axes and for which a dextro–laevo conversion was obtained by the application of an electric field (Futama & Pepinsky, 1962).

The crystal structure of ALS was first solved by X-ray diffraction by Vedam, Okaya & Pepinsky (1960), using isotropic thermal parameters for all the atoms. They, however, made no attempt to locate the lithium ion in the structure directly, but assigned to it a probable position (0·65, 0·075, 0·23) from packing considerations. Later, a preliminary neutron diffraction study was made by Van den Hende & Boutin (1963) who reported the coordinates of the hydrogen atoms. The lithium ion, however, was not located, probably because of insufficient data and also because of the small neutron scattering cross-section for the most abundant isotope of the lithium ion. From considerations of the angular dependence of $^7$Li (nuclear magnetic resonance study of the crystal), Gavrilova-Podolskaya (1966) concluded that the lithium ion occupies the position $(\frac{1}{2}, \frac{1}{2}, \frac{1}{2})$.

## Experimental

In the course of the X-ray analysis of some ferro- and piezo-electric crystals, the authors constructed a three-dimensional model of the structure of ALS and found that the positions assigned to the lithium ion by the earlier workers were not possible. The proposed positions were too close to the heavy selenium atoms and